

# Two-body charmed baryon decays involving decuplet baryon in the quark-diagram scheme

Y.K. Hsiao,<sup>1,\*</sup> Qian Yi,<sup>1</sup> Shu-Ting Cai,<sup>1</sup> and H.J. Zhao<sup>1</sup>

<sup>1</sup>*School of Physics and Information Engineering,  
Shanxi Normal University, Linfen 041004, China*

(Dated: November 25, 2020)

## Abstract

In the quark-diagram scheme, we study the charmed baryon decays of  $\mathbf{B}_c \rightarrow \mathbf{B}^*M$ , where  $\mathbf{B}_c$  is  $\Lambda_c^+$  or  $\Xi_c^{+(0)}$ , together with  $\mathbf{B}^*$  ( $M$ ) the decuplet baryon (pseudoscalar meson). It is found that only two  $W$ -exchange processes are allowed to contribute to  $\mathbf{B}_c \rightarrow \mathbf{B}^*M$ . Particularly, we predict  $\mathcal{B}(\Lambda_c^+ \rightarrow \Sigma^{*0(+)}\pi^{+(0)}) = (2.8 \pm 0.4) \times 10^{-3}$ , which respects the isospin symmetry. Besides, we take into account the  $SU(3)$  flavor symmetry breaking, in order to explain the observation of  $\mathcal{B}(\Lambda_c^+ \rightarrow \Sigma^{*+}\eta)$ . For the decays involving  $\Delta^{++}(uuu)$ , we predict  $\mathcal{B}(\Lambda_c^+ \rightarrow \Delta^{++}\pi^-, \Xi_c^+ \rightarrow \Delta^{++}K^-) = (7.0 \pm 1.4, 13.5 \pm 2.7) \times 10^{-4}$  as the largest branching fractions in the singly Cabibbo-suppressed  $\Lambda_c^+, \Xi_c^+ \rightarrow \mathbf{B}^*M$  decay channels, respectively, which are accessible to the LHCb, BELLEII and BESIII experiments.

---

\* yukuohsiao@gmail.com

## I. INTRODUCTION

To determine the mass and lifetime of the  $\Lambda_b$  baryon,  $\Lambda_c^+$  is often taken as the final state in the  $\Lambda_b$  decays [1], which involves the favored Cabibbo-Kobayashi-Maskawa (CKM) matrix elements for bigger branching fractions. With the higher precision in the recent years [2, 3], the subsequent  $\Lambda_c^+ \rightarrow pK^-\pi^+$  decay has helped to make more accurate observations for the  $\Lambda_b$  decays, which receives the significant contribution from  $\Lambda_c^+ \rightarrow \Delta^{++}K^-, \Delta^{++} \rightarrow p\pi^+$ . Similarly, one uses  $\Xi_b^0 \rightarrow \Xi_c^+\pi^-$  to determine the  $\Xi_b^0$  lifetime, whereas we find that the subsequent process  $\Xi_c^+ \rightarrow pK^-\pi^+$  and its resonant contribution from  $\Xi_c^+ \rightarrow \Delta^{++}K^-, \Delta^{++} \rightarrow p\pi^+$  have not been well studied yet [1]. Therefore,  $\mathbf{B}_c \rightarrow \mathbf{B}^*M$  plays the key role in the precision measurements for the multi-body decays of beauty and charm baryons, where  $\mathbf{B}_c = (\Lambda_c^+, \Xi_c^{+(0)})$ ,  $\mathbf{B}^*$  the decouplet baryon and  $M$  the meson state, such as  $\Lambda_c^+(\Xi_c^+) \rightarrow \Delta^{++}K^-$ .

The  $\mathbf{B}_c \rightarrow \mathbf{B}^*M$  decays are not richly observed. Therefore, it is still unclear how the  $\mathbf{B}_c \rightarrow \mathbf{B}^*M, \mathbf{B}^* \rightarrow \mathbf{B}M'$  decays mix with the non-resonant contributions to  $\mathbf{B}_c \rightarrow \mathbf{B}MM'$ . In addition,  $\mathbf{B}_c \rightarrow \mathbf{B}V, V \rightarrow MM'$  with  $V$  the vector meson causes more complicated mixtures [1]. The  $SU(3)$  flavor ( $SU(3)_f$ ) symmetry has been widely applied to the charmed baryon decays [4–16]. By well explaining the data, the flavor symmetry does not appear to be severely broken in  $\mathbf{B}_c \rightarrow \mathbf{B}M$  [17], where  $\mathbf{B}$  denotes the octet baryon. By contrast,  $\mathcal{B}(\Lambda_c^+ \rightarrow \Sigma^{*+}\eta)$  not well interpreted by the  $SU(3)_f$  symmetry might hint the broken effect in  $\mathbf{B}_c \rightarrow \mathbf{B}^*M$  [7], which could be as large as that in the  $D$  meson decays [18–21].

For a better understanding of the hadronization in  $\mathbf{B}_c \rightarrow \mathbf{B}^*M$ , there have been some theoretical attempts, which are in terms of the pole model, quark model and irreducible  $SU(3)$  flavor ( $SU(3)_f$ ) symmetry [4–7, 22–24]. Particularly, the quark-diagram scheme with the topological  $SU(3)_f$  symmetry provides a clear picture for the decay processes [17, 25–27]. Due to the fact that  $\mathbf{B}^*$  is a spin-3/2 baryon with totally symmetric quark contents, it can be shown that the topological diagrams involving the flavor anti-symmetric quark pair in  $\mathbf{B}^*$  are forbidden or suppressed. Therefore, we purpose to use the quark-diagram scheme to relate all possible  $\mathbf{B}_c \rightarrow \mathbf{B}^*M$  decay channels. With the existing data, we will perform the numerical analysis, and determine different topological contributions. We can hence test the validity of the topological scheme, which involves the  $SU(3)_f$  symmetry and its broken effect. Furthermore, we will give predictions for  $\mathcal{B}(\mathbf{B}_c \rightarrow \mathbf{B}^*M)$  to be compared to the future measurements, which can help to clarify how  $\mathbf{B}_c \rightarrow \mathbf{B}^*M, \mathbf{B}^* \rightarrow \mathbf{B}M'$  mixes

with  $\mathbf{B}_c \rightarrow \mathbf{B}V, V \rightarrow MM'$  and the non-resonant configuration in  $\mathbf{B}_c \rightarrow \mathbf{B}MM'$ .

## II. FORMALISM

### A. Effective Hamiltonian in the flavor symmetry

To study the two-body charmed baryon decays, the corresponding quark-level effective Hamiltonian is given by [28]

$$\mathcal{H}_{eff} = \frac{G_F}{\sqrt{2}} \sum_{i=1,2} c_i (\lambda_a O_i^a + \lambda_p O_i^p + \lambda_c O_i^c), \quad (1)$$

with  $\lambda_{(a,p,c)} \equiv (V_{cs}^* V_{ud}, V_{cp}^* V_{up}, V_{cd}^* V_{us})$  and  $p = (d, s)$ , where  $G_F$  is the Fermi constant, and  $c_i$  the Wilson coefficients. The current-current operators  $O_i^{(a,p,c)}$  are written as

$$\begin{aligned} O_1^a &= (\bar{u}d)(\bar{s}c), \quad O_2^a = (\bar{u}_\beta d_\alpha)(\bar{s}_\alpha c_\beta), \\ O_1^p &= (\bar{u}p)(\bar{p}c), \quad O_2^p = (\bar{u}_\beta p_\alpha)(\bar{p}_\alpha c_\beta), \\ O_1^c &= (\bar{u}s)(\bar{d}c), \quad O_2^c = (\bar{u}_\beta s_\alpha)(\bar{d}_\alpha c_\beta), \end{aligned} \quad (2)$$

where  $(\bar{q}_1 q_2) = \bar{q}_1 \gamma_\mu (1 - \gamma_5) q_2$ , and the subscripts  $(\alpha, \beta)$  denote the color indices. With  $s_c \equiv \sin \theta_c \simeq 0.22$ , where  $\theta_c$  denotes the Cabibbo angle for the quark-mixing in the weak interaction, the decays with  $|\lambda_{(a,p,c)}| \simeq (1, s_c, s_c^2)$  are regarded as the Cabibbo-allowed (CA), singly Cabibbo-suppressed (SCS) and doubly Cabibbo-suppressed (DCS) processes, respectively.

For the lowest-lying anti-triplet charmed baryon states  $\Xi_c^0, \Xi_c^+$  and  $\Lambda_c^+$  that consist of  $(ds - sd)c, (su - us)c$  and  $(ud - du)c$ , respectively, we present them as

$$\mathbf{B}_c = \begin{pmatrix} 0 & \Lambda_c^+ & \Xi_c^+ \\ -\Lambda_c^+ & 0 & \Xi_c^0 \\ -\Xi_c^+ & -\Xi_c^0 & 0 \end{pmatrix}. \quad (3)$$

The pseudoscalar meson states are given by

$$M = \begin{pmatrix} \frac{1}{\sqrt{2}}(\pi^0 + c\phi\eta + s\phi\eta') & \pi^- & K^- \\ \pi^+ & \frac{-1}{\sqrt{2}}(\pi^0 - c\phi\eta - s\phi\eta') & \bar{K}^0 \\ K^+ & K^0 & -s\phi\eta + c\phi\eta' \end{pmatrix}, \quad (4)$$

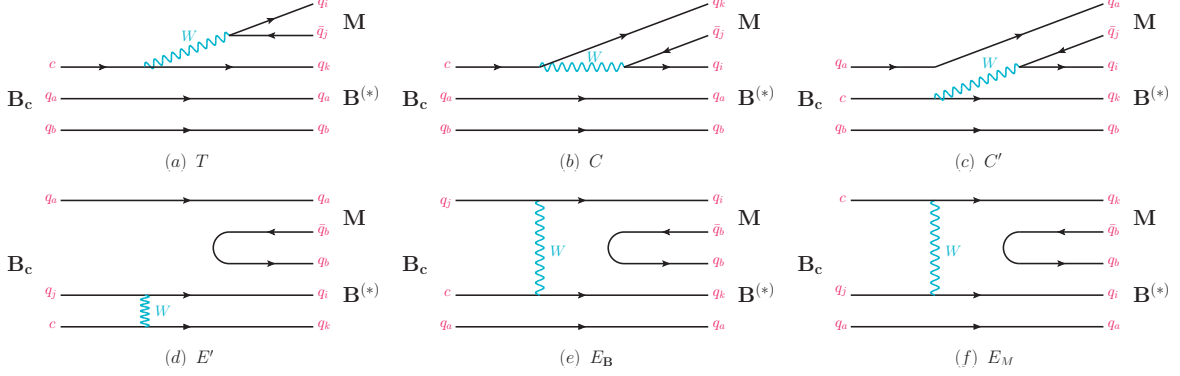


FIG. 1. Topological diagrams for the  $\mathbf{B}_c \rightarrow \mathbf{B}^{(*)}M$  decays.

where  $(\eta, \eta')$  mix with  $\eta_q = \sqrt{1/2}(u\bar{u} + d\bar{d})$  and  $\eta_s = s\bar{s}$ . The mixing angle  $\phi = (39.3 \pm 1.0)^\circ$  in  $(s\phi, c\phi) \equiv (\sin \phi, \cos \phi)$  comes from the mixing matrix, given by [29]

$$\begin{pmatrix} \eta \\ \eta' \end{pmatrix} = \begin{pmatrix} \cos \phi & -\sin \phi \\ \sin \phi & \cos \phi \end{pmatrix} \begin{pmatrix} \eta_q \\ \eta_s \end{pmatrix}. \quad (5)$$

The decuplet baryons are written as

$$\mathbf{B}^* = \frac{1}{\sqrt{3}} \left( \begin{pmatrix} \sqrt{3}\Delta^{++} & \Delta^+ & \Sigma^{*+} \\ \Delta^+ & \Delta^0 & \frac{\Sigma^{*0}}{\sqrt{2}} \\ \Sigma^{*+} & \frac{\Sigma^{*0}}{\sqrt{2}} & \Xi^{*0} \end{pmatrix}, \begin{pmatrix} \Delta^+ & \Delta^0 & \frac{\Sigma^{*0}}{\sqrt{2}} \\ \Delta^0 & \sqrt{3}\Delta^- & \Sigma^{*-} \\ \frac{\Sigma^{*0}}{\sqrt{2}} & \Sigma^{*-} & \Xi^{*-} \end{pmatrix}, \begin{pmatrix} \Sigma^{*+} & \frac{\Sigma^{*0}}{\sqrt{2}} & \Xi^{*0} \\ \frac{\Sigma^{*0}}{\sqrt{2}} & \Sigma^{*-} & \Xi^{*-} \\ \Xi^{*0} & \Xi^{*-} & \sqrt{3}\Omega^- \end{pmatrix} \right). \quad (6)$$

By neglecting the Lorentz indices,  $\mathcal{H}_{eff}$  for the  $c \rightarrow q_i \bar{q}_j q_k$  transition can be presented with the tensor notation,  $H_j^{ki}$ , and the nonzero entries are given by [27]

$$H_2^{31} = \lambda_a, H_2^{21} = \lambda_d, H_3^{31} = \lambda_s, H_3^{21} = \lambda_c. \quad (7)$$

## B. The quark-diagram scheme

In the quark-diagram scheme, there exist six different topological diagrams for the  $\mathbf{B}_c \rightarrow \mathbf{B}^{(*)}M$  decays, as drawn in Figs. 1(a,b,c) and 1(d,e,f), parameterized as the topological amplitudes  $(T, C, C')$  and  $(E', E_B, E_M)$ , respectively [17]. More explicitly,  $T$  and  $C^{(l)}$  proceed with the  $W$ -boson emission ( $W_{EM}$ ). By exchanging the  $W$  boson ( $W_{EX}$ ), it gives rise to  $E'$  and  $E_{B(M)}$ . Since only  $(T, C)$  can be decomposed of two separate matrix elements based on the factorization, that is,  $(T, C) \propto \langle M | \bar{q}_1 q_2 | 0 \rangle \langle \mathbf{B}^{(*)} | \bar{q}_3 c | \mathbf{B}_c \rangle$  [30], one classifies  $(T, C)$  and  $(C', E', E_{M,B})$  as the factorizable and non-factorizable amplitudes, respectively.

Furthermore, it is found in Figs. 1(a,b) that  $\mathbf{B}_c$  with  $(q_a q_b - q_b q_a)c$  cannot be turned into  $\mathbf{B}^*(q_a q_b q_{k(i)})$ , where  $q_a q_b q_{k(i)}$  are totally symmetric, such that  $(T, C)$  give no contributions to  $\mathbf{B}_c \rightarrow \mathbf{B}^* M$ . Thus, the  $\mathbf{B}_c \rightarrow \mathbf{B}^* M$  decays are purely non-factorizable processes. In addition,  $C'$  and  $E'$  are suppressed in  $\mathbf{B}_c \rightarrow \mathbf{B}^* M$  [25], which is in accordance with the Körner-Pati-Woo theorem [31]. With the current-current structure of  $(\bar{q}_i q_j)_{V-A}(\bar{q}_k c)_{V-A}$  in Eq. (2),  $q_i$  and  $q_k$  are color anti-symmetric. When combined as the constituents of the baryon,  $q_{i,k}$  are flavor anti-symmetric, such that the topological diagrams  $(C', E')$  in Figs. 1(c,d) contribute to  $\mathbf{B}_c \rightarrow \mathbf{B} M$ , instead of  $\mathbf{B}_c \rightarrow \mathbf{B}^* M$ . Consequently, we are left with the  $W_{\text{EX}}$  topological diagrams  $(E_{\mathbf{B}}, E_M)$  in Figs. 1(e,f) for  $\mathbf{B}_c \rightarrow \mathbf{B}^* M$ .

To proceed, we derive the amplitudes as  $\mathcal{A}(\mathbf{B}_c \rightarrow \mathbf{B}^* M) = (G_F/\sqrt{2})T(\mathbf{B}_c \rightarrow \mathbf{B}^* M)$ . Explicitly, the  $T$  amplitudes ( $T$ -amps) read [17, 25, 27]

$$T(\mathbf{B}_c \rightarrow \mathbf{B}^* M) = E_{\mathbf{B}}^{(s)}(\mathbf{B}_c)^{ja} H_j^{ki}(\mathbf{B}^*)_{kab}(M)_i^b + E_M^{(s)}(\mathbf{B}_c)^{ja} H_j^{ki}(\mathbf{B}^*)_{iab}(M)_k^b, \quad (8)$$

where the parameters  $E_{\mathbf{B},M}^{(s)}$  correspond to the topological diagrams in Figs. 1e and 1f, respectively. The  $W_{\text{EX}}$  decay process needs an additional quark pair from  $g \rightarrow q\bar{q}$ , where  $q\bar{q}$  could be  $u\bar{u}$ ,  $d\bar{d}$  or  $s\bar{s}$ . To take into account the broken  $SU(3)_f$  symmetry,  $E_{\mathbf{B}(M)}$  with  $g \rightarrow s\bar{s}$  can be more specifically denoted by  $E_{\mathbf{B}(M)}^s$ . Under the exact  $SU(3)_f$  symmetry, it leads to  $E_{\mathbf{B}(M)}^s = E_{\mathbf{B}(M)}$  [26]. In Tables I, II and III, we present the full expansions of  $T(\mathbf{B}_c \rightarrow \mathbf{B}^* M)$  for the CA, SCS and DCS decay modes, respectively. For the branching fractions, we use the equation for the two-body decays, given by [1]

$$\begin{aligned} \mathcal{B}(\mathbf{B}_c \rightarrow \mathbf{B}^* M) &= \frac{G_F^2 |\vec{p}_{\mathbf{B}^*}| \tau_{\mathbf{B}_c}}{16\pi m_{\mathbf{B}_c}^2} |T(\mathbf{B}_c \rightarrow \mathbf{B}^* M)|^2, \\ |\vec{p}_{\mathbf{B}^*}| &= \frac{\sqrt{(m_{\mathbf{B}_c}^2 - m_{\pm}^2)(m_{\mathbf{B}_c}^2 - m_{\mp}^2)}}{2m_{\mathbf{B}_c}}, \end{aligned} \quad (9)$$

with  $m_{\pm} = m_{\mathbf{B}^*} \pm m_M$ , where  $\tau_{\mathbf{B}_c}$  stands for the  $\mathbf{B}_c$  baryon lifetime.

### III. NUMERICAL ANALYSIS AND DISCUSSIONS

In the numerical analysis, we adopt the Cabibbo-Kobayashi-Maskawa (CKM) matrix elements as [1]

$$(V_{cs}, V_{ud}, V_{us}, V_{cd}) = (1 - \lambda^2/2, 1 - \lambda^2/2, \lambda, -\lambda), \quad (10)$$

with  $\lambda = s_c = 0.22453 \pm 0.00044$  in the Wolfenstein parameterization. Besides, the  $\mathbf{B}_c$  and  $\mathbf{B}^*$  masses, together with the lifetime for  $\mathbf{B}_c$ , are adopted from the PDG [1]. We perform

a minimum  $\chi^2$ -fit with  $\chi^2 = \sum(\mathcal{B}_{th} - \mathcal{B}_{ex})^2/\sigma_{ex}^2$ , where  $\mathcal{B}_{th(ex)}$  represents the theoretical (experimental) input of the branching ratio, and  $\sigma_{ex}$  the experimental error. We calculate  $\mathcal{B}_{th}$  with the equation in Eq. (9), together with  $(\mathcal{B}_{ex}, \sigma_{ex})$  from Table I. Note that  $\mathcal{B}(\Xi_c^+ \rightarrow \Sigma^{*+} \bar{K}^0, \Xi^{*0} \pi^+)$  are not involved in the fit.

We use two scenarios for the global fit. In the first scenario ( $S1$ ), we take  $E_{\mathbf{B}(M)}^s = E_{\mathbf{B}(M)}$  under the exact  $SU(3)_f$  symmetry. Since  $E_{\mathbf{B}}$  and  $E_M$  are complex numbers, it leads to three independent parameters, given by

$$|E_{\mathbf{B}}|, |E_M|e^{i\delta_{E_M}}, \quad (11)$$

where  $E_{\mathbf{B}}$  is set to be real, and  $\delta_{E_M}$  is a relative strong phase. Using the  $\chi^2$ -fit, we extract that

$$\begin{aligned} (|E_{\mathbf{B}}|, |E_M|) &= (0.41 \pm 0.03, 0.34 \pm 0.03) \text{ GeV}^3, \\ \delta_{E_M} &= (180.0 \pm 35.8)^\circ, \end{aligned} \quad (12)$$

with  $\chi^2/n.d.f = 4.5$ , where  $n.d.f = 1$  is the number of the degrees of freedom. For  $\delta_{E_M}$ , its information is from  $\mathcal{B}(\Lambda_c^+ \rightarrow \Sigma^{*+} \eta)$ . Although  $\delta_{E_M} = 180^\circ$  has induced the largest positive interference between  $E_{\mathbf{B}}$  and  $E_M$ , our result of  $\mathcal{B}(\Lambda_c^+ \rightarrow \Sigma^{*+} \eta) = (5.3 \pm 0.7) \times 10^{-3}$  is still

TABLE I. Cabibbo-allowed  $\mathbf{B}_c \rightarrow \mathbf{B}^* M$  decays.

Decay modes	$T$ -amp	$10^3 \mathcal{B} (S1, S2)$ [our work]	$10^3 \mathcal{B} (S_{pm}, S_{em})$ [7]	$10^3 \mathcal{B}_{ex}$ [1, 32]
$\Lambda_c^+ \rightarrow \Delta^{++} K^-$	$-\lambda_a E_M$	(12.0 $\pm$ 2.2, 11.7 $\pm$ 2.3)	(15.3 $\pm$ 2.4, 12.4 $\pm$ 1.0)	10.8 $\pm$ 2.5
$\Lambda_c^+ \rightarrow \Delta^+ \bar{K}^0$	$-\lambda_a \frac{1}{\sqrt{3}} E_M$	(4.0 $\pm$ 0.7, 3.9 $\pm$ 0.8)	(5.1 $\pm$ 0.8, 4.1 $\pm$ 0.3)	—
$\Lambda_c^+ \rightarrow \Sigma^{*0} \pi^+$	$-\lambda_a \frac{1}{\sqrt{6}} E_{\mathbf{B}}$	(2.9 $\pm$ 0.4, 2.8 $\pm$ 0.4)	(2.2 $\pm$ 0.4, 2.1 $\pm$ 0.2)	—
$\Lambda_c^+ \rightarrow \Sigma^{*+} \pi^0$	$-\lambda_a \frac{1}{\sqrt{6}} E_{\mathbf{B}}$	(2.9 $\pm$ 0.4, 2.8 $\pm$ 0.4)	(2.2 $\pm$ 0.4, 2.1 $\pm$ 0.2)	—
$\Lambda_c^+ \rightarrow \Sigma^{*+} \eta$	$-\lambda_a \frac{1}{\sqrt{6}} (E_{\mathbf{B}} c\phi - \sqrt{2} E_M^{(s)} s\phi)$	(5.3 $\pm$ 0.8, 7.3 $\pm$ 1.5)	(3.1 $\pm$ 0.6, 6.2 $\pm$ 0.5)	9.1 $\pm$ 2.0
$\Lambda_c^+ \rightarrow \Sigma^{*+} \eta'$	$-\lambda_a \frac{1}{\sqrt{6}} (E_{\mathbf{B}} s\phi + \sqrt{2} E_M^{(s)} c\phi)$	(0, 0)	—	—
$\Lambda_c^+ \rightarrow \Xi^{*0} K^+$	$-\lambda_a \frac{1}{\sqrt{3}} E_{\mathbf{B}}$	(3.9 $\pm$ 0.6, 3.9 $\pm$ 0.6)	(1.0 $\pm$ 0.2, 4.1 $\pm$ 0.3)	4.3 $\pm$ 0.9
$\Xi_c^0 \rightarrow \Sigma^{*+} K^-$	$\lambda_a \frac{1}{\sqrt{3}} E_M$	(1.8 $\pm$ 0.3, 1.7 $\pm$ 0.3)	(3.1 $\pm$ 0.5, 2.3 $\pm$ 0.2)	—
$\Xi_c^0 \rightarrow \Sigma^{*0} \bar{K}^0$	$\lambda_a \frac{1}{\sqrt{6}} E_M$	(0.9 $\pm$ 0.2, 0.9 $\pm$ 0.2)	(1.6 $\pm$ 0.2, 1.2 $\pm$ 0.1)	—
$\Xi_c^0 \rightarrow \Xi^{*-} \pi^+$	$\lambda_a \frac{1}{\sqrt{3}} E_{\mathbf{B}}$	(2.6 $\pm$ 0.4, 2.5 $\pm$ 0.4)	(2.8 $\pm$ 0.5, 2.3 $\pm$ 0.2)	—
$\Xi_c^0 \rightarrow \Xi^{*0} \pi^0$	$\lambda_a \frac{1}{\sqrt{6}} E_{\mathbf{B}}$	(1.3 $\pm$ 0.2, 1.3 $\pm$ 0.2)	(1.4 $\pm$ 0.2, 1.2 $\pm$ 0.1)	—
$\Xi_c^0 \rightarrow \Xi^{*0} \eta$	$\lambda_a \frac{1}{\sqrt{6}} (E_{\mathbf{B}} c\phi - \sqrt{2} E_M^{(s)} s\phi)$	(2.4 $\pm$ 0.4, 3.4 $\pm$ 0.7)	(2.1 $\pm$ 0.4, 3.5 $\pm$ 0.3)	—
$\Xi_c^0 \rightarrow \Xi^{*0} \eta'$	$\lambda_a \frac{1}{\sqrt{6}} (E_{\mathbf{B}} s\phi + \sqrt{2} E_M^{(s)} c\phi)$	(0.01 $\pm$ 0.04, 0.08 $\pm$ 0.10)	—	—
$\Xi_c^0 \rightarrow \Omega^- K^+$	$\lambda_a E_{\mathbf{B}}^{(s)}$	(4.8 $\pm$ 0.7, 4.8 $\pm$ 0.7)	(2.3 $\pm$ 0.5, 7.0 $\pm$ 0.6)	4.2 $\pm$ 1.0
$\Xi_c^+ \rightarrow \Sigma^{*+} \bar{K}^0$	0	0	0	28.6 $\pm$ 16.8
$\Xi_c^+ \rightarrow \Xi^{*0} \pi^+$	0	0	0	< 4.0

shown to be in tension with the observation of  $(9.1 \pm 2.0) \times 10^{-3}$ . Sizeably, it adds 3.6 to the total  $\chi^2$  value.

Since  $\Lambda_c^+ \rightarrow \Sigma^{*+}\eta$  is in association with  $|E_M^s|$ , the tension hints the broken  $SU(3)_f$  symmetry, where  $|E_M^s|$  is not equal to  $|E_M|$ . On the other hand,  $\mathcal{B}(\Xi_c^0 \rightarrow \Omega^- K^+)$  is fitted to agree with the data, indicating that  $|E_{\mathbf{B}}^s|$  is not deviating from  $|E_{\mathbf{B}}|$ . Currently, the data points are not sufficient for an independent extraction of  $|E_M^s|$ . We hence adopt the numerical results from the two-body  $D$  meson decays, where the similar  $W_{\text{EX}}$  contributions have been found to induce the severe  $SU(3)_f$  symmetry breaking [18–21]. In the second scenario ( $S2$ ), we take  $|E_M^s| = n_q \times |E_M|$  and  $|E_{\mathbf{B}}^s| \simeq |E_{\mathbf{B}}|$ , with  $n_q = 1.4$  adopted from [21]. Consequently, we obtain

$$\begin{aligned} (|E_{\mathbf{B}}|, |E_M|) &= (0.40 \pm 0.03, 0.34 \pm 0.03) \text{ GeV}^3, \\ \delta_{E_M} &= (180.0 \pm 46.8)^\circ, \end{aligned} \quad (13)$$

where  $\chi^2/n.d.f$  is reduced as 1.3. As the demonstration, we obtain  $\mathcal{B}(\Lambda_c^+ \rightarrow \Sigma^{*+}\eta) = (7.3 \pm 1.5) \times 10^{-3}$ , which alleviates the deviation from the observation. With the fit values of  $(|E_{\mathbf{B}}|, |E_M|, \delta_{E_M})$  in  $S1$  and  $S2$ , we present the branching ratios of the  $\mathbf{B}_c \rightarrow \mathbf{B}^*M$  decays in Tables I, II and III, along with the recent theoretical results for comparison.

We get some useful relations in the quark-diagram scheme. For example, we find out three triangle sum rules for  $\mathbf{B}_c \rightarrow \Delta\pi$ , given by

$$\begin{aligned} T(\Lambda_c^+ \rightarrow \Delta^0\pi^+) - T(\Lambda_c^+ \rightarrow \Delta^{++}\pi^-) - \sqrt{6}T(\Lambda_c^+ \rightarrow \Delta^+\pi^0) &= 0, \\ T(\Xi_c^+ \rightarrow \Delta^0\pi^+) - T(\Xi_c^+ \rightarrow \Delta^{++}\pi^-) - \sqrt{6}T(\Xi_c^+ \rightarrow \Delta^+\pi^0) &= 0, \\ T(\Xi_c^0 \rightarrow \Delta^+\pi^-) - T(\Xi_c^0 \rightarrow \Delta^-\pi^+) - \sqrt{6}T(\Xi_c^0 \rightarrow \Delta^0\pi^0) &= 0. \end{aligned} \quad (14)$$

Besides, we obtain

$$\begin{aligned} T(\Lambda_c^+ \rightarrow \Delta^+ K^0, \Delta^0 K^+) &= 0, \\ T(\Xi_c^+ \rightarrow \Sigma^{*+} \bar{K}^0, \Xi^{*0} \pi^+) &= 0, \end{aligned} \quad (15)$$

as the consequence of  $C'$  being set to give no contribution to  $\mathbf{B}_c \rightarrow \mathbf{B}^*M$ . Indeed,  $C'$  is the only topology that takes part in the decays in Eq. (15), but suppressed due to the Körner-Pati-Woo theorem [31]. According to the other theoretical calculations [6, 7, 22–24],  $\mathcal{B}(\Xi_c^+ \rightarrow \Sigma^{*+} \bar{K}^0, \Xi^{*0} \pi^+) = 0$  is also predicted, which supports that  $C' = 0$ . Experimentally,  $\mathcal{B}_{ex}(\Xi_c^+ \rightarrow \Sigma^{*+} \bar{K}^0, \Xi^{*0} \pi^+)$  in Table II can be used to test the suppression. With  $\mathcal{B}(\Xi_c^+ \rightarrow$

$\Xi^{*0}\pi^+/\mathcal{B}(\Xi_c^+ \rightarrow \Xi^-\pi^+\pi^+) < 0.1$  and  $\mathcal{B}(\Xi_c^+ \rightarrow \Xi^-\pi^+\pi^+) = (2.86 \pm 1.21 \pm 0.38) \times 10^{-2}$  [1, 32], we determine  $\mathcal{B}_{ex}(\Xi_c^+ \rightarrow \Xi^{*0}\pi^+) < 4.0 \times 10^{-3}$ , which can be seen as the non-observation to agree with  $T(\Xi_c^+ \rightarrow \Xi^{*0}\pi^+) = 0$ . However,  $\mathcal{B}_{ex}(\Xi_c^+ \rightarrow \Sigma^{*+}\bar{K}^0) = (2.9 \pm 1.7) \times 10^{-2}$  seems to disagree with the prediction of  $\mathcal{B}(\Xi_c^+ \rightarrow \Sigma^{*+}\bar{K}^0) = 0$ , despite of the large uncertainty. While the Körner-Pati-Woo theorem is regarded as a tree-level approximation, allowing possible corrections to  $C'$  and  $E'$ , we need more accurate observations to test if  $C'(E') = 0$ .

Uniquely, the decuplet baryon can contain three identical quarks, denoted by  $\mathbf{B}^*(qqq)$ , which leads to an additional weight factor of  $\sqrt{3}$  among the decuplet baryons in Eq. (6). The factor can be considered as the main reason why  $\Lambda_c^+ \rightarrow \Delta^{++}K^-$  and  $\Xi_c^0 \rightarrow \Omega^-K^+$  are measured with the largest branching fractions in the CA decay channels of  $\Lambda_c^+, \Xi_c^0 \rightarrow \mathbf{B}^*M$ , respectively. Accordingly, the  $T$ -amps with  $\mathbf{B}^*(qqq)$  are listed as

$$T(\Lambda_c^+ \rightarrow \Delta^{++}K^-, \Delta^{++}\pi^-) = -(\lambda_a, \lambda_d) E_M,$$

TABLE II. Singly Cabibbo-suppressed  $\mathbf{B}_c \rightarrow \mathbf{B}^*M$  decays.

Decay modes	$T$ -amp	$10^4\mathcal{B}(S1, S2)$ [our work]	$10^4\mathcal{B}(S_{pm}, S_{em})$ [7]
$\Lambda_c^+ \rightarrow \Delta^{++}\pi^-$	$-\lambda_d E_M$	$(7.2 \pm 1.3, 7.0 \pm 1.4)$	$(12.5 \pm 2.0, 6.6 \pm 0.6)$
$\Lambda_c^+ \rightarrow \Delta^+\pi^0$	$-\lambda_d \frac{1}{\sqrt{6}}(E_{\mathbf{B}} - E_M)$	$(5.8 \pm 0.9, 5.6 \pm 1.1)$	$(8.3 \pm 1.3, 4.4 \pm 0.4)$
$\Lambda_c^+ \rightarrow \Delta^0\pi^+$	$-\lambda_d \frac{1}{\sqrt{3}}E_{\mathbf{B}}$	$(3.5 \pm 0.5, 3.3 \pm 0.5)$	$(4.2 \pm 0.7, 2.2 \pm 0.2)$
$\Lambda_c^+ \rightarrow \Delta^+\eta$	$-\lambda_d \frac{1}{\sqrt{6}}(E_{\mathbf{B}} + E_M)c\phi$	$(0.03 \pm 0.28, 0.02 \pm 0.45)$	—
$\Lambda_c^+ \rightarrow \Delta^+\eta'$	$-\lambda_d \frac{1}{\sqrt{6}}(E_{\mathbf{B}} + E_M)s\phi$	$(0.01 \pm 0.09, 0.01 \pm 0.15)$	—
$\Lambda_c^+ \rightarrow \Sigma^{*+}K^0$	$-\lambda_d \frac{1}{\sqrt{3}}E_M^{(s)}$	$(1.8 \pm 0.4, 3.5 \pm 0.7)$	$(1.3 \pm 0.2, 2.2 \pm 0.2)$
$\Lambda_c^+ \rightarrow \Sigma^{*0}K^+$	$-\lambda_d \frac{1}{\sqrt{6}}E_{\mathbf{B}}^{(s)}$	$(1.3 \pm 0.2, 1.3 \pm 0.2)$	$(0.7 \pm 0.1, 1.1 \pm 0.1)$
$\Xi_c^0 \rightarrow \Delta^+K^-$	$-\lambda_s \frac{1}{\sqrt{3}}E_M$	$(1.1 \pm 0.2, 1.0 \pm 0.2)$	$(3.0 \pm 0.5, 1.2 \pm 0.1)$
$\Xi_c^0 \rightarrow \Delta^0\bar{K}^0$	$-\lambda_s \frac{1}{\sqrt{3}}E_M$	$(1.1 \pm 0.2, 1.0 \pm 0.2)$	$(3.0 \pm 0.5, 1.2 \pm 0.1)$
$\Xi_c^0 \rightarrow \Sigma^{*-}\pi^+$	$\frac{1}{\sqrt{3}}(\lambda_d E_{\mathbf{B}} - \lambda_s E_{\mathbf{B}})$	$(6.1 \pm 0.9, 5.8 \pm 0.9)$	$(9.9 \pm 1.6, 4.9 \pm 0.4)$
$\Xi_c^0 \rightarrow \Sigma^{*+}\pi^-$	$\lambda_d \frac{1}{\sqrt{3}}E_M$	$(1.0 \pm 0.2, 1.0 \pm 0.2)$	$(2.5 \pm 0.4, 1.2 \pm 0.1)$
$\Xi_c^0 \rightarrow \Sigma^{*0}\pi^0$	$\frac{1}{\sqrt{12}}[\lambda_d(E_{\mathbf{B}} - E_M) - \lambda_s E_{\mathbf{B}}]$	$(3.1 \pm 0.4, 2.9 \pm 0.5)$	$(5.6 \pm 0.9, 2.8 \pm 0.2)$
$\Xi_c^0 \rightarrow \Sigma^{*0}\eta$	$\frac{1}{\sqrt{12}}[\lambda_d(E_{\mathbf{B}} + E_M)c\phi + \lambda_s(\sqrt{2}E_M^{(s)}s\phi - E_{\mathbf{B}}c\phi)]$	$(0.9 \pm 0.2, 1.2 \pm 0.3)$	$(1.1 \pm 0.2, 0.9 \pm 0.1)$
$\Xi_c^0 \rightarrow \Sigma^{*0}\eta'$	$\frac{1}{\sqrt{12}}[\lambda_d(E_{\mathbf{B}} + E_M)s\phi - \lambda_s(\sqrt{2}E_M^{(s)}c\phi + E_{\mathbf{B}}s\phi)]$	$(0.004 \pm 0.120, 0.050 \pm 0.250)$	—
$\Xi_c^0 \rightarrow \Xi^{*0}K^0$	$\frac{1}{\sqrt{3}}\lambda_d E_M^{(s)}$	$(0.8 \pm 0.2, 1.6 \pm 0.4)$	$(0.9 \pm 0.2, 1.2 \pm 0.1)$
$\Xi_c^0 \rightarrow \Xi^{*-}K^+$	$\frac{1}{\sqrt{3}}(\lambda_d E_{\mathbf{B}}^{(s)} - \lambda_s E_{\mathbf{B}}^{(s)})$	$(4.6 \pm 0.7, 4.6 \pm 0.7)$	$(3.6 \pm 0.6, 4.9 \pm 0.4)$
$\Xi_c^+ \rightarrow \Delta^{++}K^-$	$-\lambda_s E_M$	$(13.8 \pm 2.5, 13.5 \pm 2.7)$	$(35.0 \pm 5.7, 14.6 \pm 1.2)$
$\Xi_c^+ \rightarrow \Delta^+\bar{K}^0$	$-\lambda_s \frac{1}{\sqrt{3}}E_M$	$(4.6 \pm 0.8, 4.5 \pm 0.9)$	$(11.7 \pm 1.9, 4.9 \pm 0.4)$
$\Xi_c^+ \rightarrow \Sigma^{*+}\pi^0$	$-\lambda_s \frac{1}{\sqrt{6}}E_{\mathbf{B}}$	$(3.4 \pm 0.5, 3.2 \pm 0.5)$	$(4.8 \pm 0.8, 2.4 \pm 0.2)$
$\Xi_c^+ \rightarrow \Sigma^{*0}\pi^+$	$-\lambda_s \frac{1}{\sqrt{6}}E_{\mathbf{B}}$	$(3.4 \pm 0.5, 3.2 \pm 0.5)$	$(4.8 \pm 0.8, 2.4 \pm 0.2)$
$\Xi_c^+ \rightarrow \Sigma^{*+}\eta$	$-\lambda_s \frac{1}{\sqrt{6}}(E_{\mathbf{B}}c\phi - \sqrt{2}E_M^{(s)}s\phi)$	$(6.4 \pm 1.0, 9.1 \pm 1.8)$	$(8.7 \pm 1.4, 7.3 \pm 0.6)$
$\Xi_c^+ \rightarrow \Sigma^{*+}\eta'$	$-\lambda_s \frac{1}{\sqrt{6}}(E_{\mathbf{B}}s\phi + \sqrt{2}E_M^{(s)}c\phi)$	$(0.1 \pm 0.3, 0.6 \pm 0.8)$	—
$\Xi_c^+ \rightarrow \Xi^{*0}K^+$	$-\lambda_s \frac{1}{\sqrt{3}}E_{\mathbf{B}}^{(s)}$	$(5.0 \pm 0.8, 5.0 \pm 0.8)$	$(3.5 \pm 0.6, 4.9 \pm 0.4)$



$$\begin{aligned}
T(\Xi_c^+ \rightarrow \Delta^{++} K^-, \Delta^{++} \pi^-) &= -(\lambda_s, \lambda_c) E_M, \\
T(\Xi_c^0 \rightarrow \Omega^- K^+, \Delta^- \pi^+) &= (\lambda_a, -\lambda_c) E_{\mathbf{B}}.
\end{aligned} \tag{16}$$

While  $\mathcal{B}(\Lambda_c^+ \rightarrow \Delta^{++} K^-)$  and  $\mathcal{B}(\Xi_c^0 \rightarrow \Omega^- K^+)$  have been observed, the other branching fractions are given by

$$\begin{aligned}
\mathcal{B}(\Lambda_c^+ \rightarrow \Delta^{++} \pi^-, \Xi_c^+ \rightarrow \Delta^{++} K^-) &= (7.0 \pm 1.4, 13.5 \pm 2.7) \times 10^{-4}, \\
\mathcal{B}(\Xi_c^+ \rightarrow \Delta^{++} \pi^-, \Xi_c^0 \rightarrow \Delta^- \pi^+) &= (7.8 \pm 1.6, 2.5 \pm 0.4) \times 10^{-5},
\end{aligned} \tag{17}$$

which are predicted as the largest branching fractions in the SCS  $\Lambda_c^+(\Xi_c^+)$  and DCS  $\Xi_c^{+(0)}$  decay channels, respectively. Here, we present our predictions of  $S2$ , which is favored by the  $\chi^2$ -fit. The equality of  $T(\Lambda_c^+ \rightarrow \Sigma^{*0} \pi^+) = T(\Lambda_c^+ \rightarrow \Sigma^{*+} \pi^0)$  corresponds to the isospin symmetry. The branching fraction, given by

$$\mathcal{B}(\Lambda_c^+ \rightarrow \Sigma^{*0(+)} \pi^{+(0)}) = (2.8 \pm 0.4) \times 10^{-3}, \tag{18}$$

can be used to test the broken effect. The decays  $\mathbf{B}_c \rightarrow \mathbf{B}^* \eta^{(\prime)}$ ,  $\Lambda_c^+ \rightarrow \Sigma^{*+} \eta$ ,  $\Xi_c^0 \rightarrow \Xi^{*0} \eta$  and  $\Xi_c^+ \rightarrow \Sigma^{*+} \eta$  have sizeable branching fractions, which is due to the constructive interferences between  $E_{\mathbf{B}}$  and  $E_M$ . However, the other branching fractions of  $\mathbf{B}_c \rightarrow \mathbf{B}^* \eta^{(\prime)}$  are typically small with the destructive interferences. Moreover, we find that  $\mathcal{B}(\Lambda_c^+ \rightarrow \Sigma^{*+} \eta') = 0$  with  $m_{\Lambda_c^+} < m_{\Sigma^{*+}} + m_{\eta'}$ .

TABLE III. Doubly Cabibbo-suppressed  $\mathbf{B}_c \rightarrow \mathbf{B}^* M$  decays.

Decay modes	$T$ -amp	$10^5 \mathcal{B} (S1, S2)$ [our work]	$10^5 \mathcal{B} (S_{pm}, S_{em})$ [7]
$\Lambda_c^+ \rightarrow \Delta^+ K^0$	0	0	0
$\Lambda_c^+ \rightarrow \Delta^0 K^+$	0	0	0
$\Xi_c^0 \rightarrow \Delta^+ \pi^-$	$-\lambda_c \frac{1}{\sqrt{3}} E_M$	$(0.6 \pm 0.1, 0.6 \pm 0.1)$	$(2.2 \pm 0.4, 0.7 \pm 0.1)$
$\Xi_c^0 \rightarrow \Delta^0 \pi^0$	$-\lambda_c \frac{1}{\sqrt{6}} (E_{\mathbf{B}} - E_M)$	$(1.5 \pm 0.2, 1.4 \pm 0.3)$	$(4.3 \pm 0.7, 1.3 \pm 0.1)$
$\Xi_c^0 \rightarrow \Delta^- \pi^+$	$-\lambda_c E_{\mathbf{B}}$	$(2.7 \pm 0.4, 2.5 \pm 0.4)$	$(6.5 \pm 1.1, 2.0 \pm 0.2)$
$\Xi_c^0 \rightarrow \Delta^0 \eta$	$-\lambda_c \frac{1}{\sqrt{6}} (E_{\mathbf{B}} + E_M) c\phi$	$(0.01 \pm 0.07, 0.01 \pm 0.12)$	—
$\Xi_c^0 \rightarrow \Delta^0 \eta'$	$-\lambda_c \frac{1}{\sqrt{6}} (E_{\mathbf{B}} + E_M) s\phi$	$(0.003 \pm 0.034, 0.003 \pm 0.055)$	—
$\Xi_c^0 \rightarrow \Sigma^{*0} K^0$	$-\lambda_c \frac{1}{\sqrt{6}} E_M^{(s)}$	$(0.2 \pm 0.1, 0.5 \pm 0.1)$	$(0.4 \pm 0.1, 0.3 \pm 0.0)$
$\Xi_c^0 \rightarrow \Sigma^{*-} K^+$	$-\lambda_c \frac{1}{\sqrt{3}} E_{\mathbf{B}}^{(s)}$	$(0.7 \pm 0.1, 0.7 \pm 0.1)$	$(0.9 \pm 0.1, 0.7 \pm 0.1)$
$\Xi_c^+ \rightarrow \Delta^{++} \pi^-$	$-\lambda_c E_M$	$(8.0 \pm 1.5, 7.8 \pm 1.6)$	$(25.5 \pm 4.4, 7.8 \pm 0.7)$
$\Xi_c^+ \rightarrow \Delta^+ \pi^0$	$-\lambda_c \frac{1}{\sqrt{6}} (E_{\mathbf{B}} - E_M)$	$(6.5 \pm 1.0, 6.3 \pm 1.2)$	$(17.0 \pm 2.9, 5.2 \pm 0.4)$
$\Xi_c^+ \rightarrow \Delta^0 \pi^+$	$-\lambda_c \frac{1}{\sqrt{3}} E_{\mathbf{B}}$	$(3.9 \pm 0.6, 3.7 \pm 0.7)$	$(8.5 \pm 1.5, 2.6 \pm 0.2)$
$\Xi_c^+ \rightarrow \Delta^+ \eta$	$-\lambda_c \frac{1}{\sqrt{6}} (E_{\mathbf{B}} + E_M) c\phi$	$(0.03 \pm 0.32, 0.03 \pm 0.52)$	—
$\Xi_c^+ \rightarrow \Delta^+ \eta'$	$-\lambda_c \frac{1}{\sqrt{6}} (E_{\mathbf{B}} + E_M) s\phi$	$(0.01 \pm 0.15, 0.01 \pm 0.24)$	—
$\Xi_c^+ \rightarrow \Sigma^{*+} K^0$	$-\lambda_c \frac{1}{\sqrt{3}} E_M^{(s)}$	$(2.1 \pm 0.4, 4.2 \pm 0.8)$	$(3.5 \pm 0.6, 2.6 \pm 0.2)$
$\Xi_c^+ \rightarrow \Sigma^{*0} K^+$	$-\lambda_c \frac{1}{\sqrt{6}} E_{\mathbf{B}}^{(s)}$	$(1.5 \pm 0.2, 1.5 \pm 0.2)$	$(1.7 \pm 0.3, 1.3 \pm 0.1)$

The approach of the irreducible  $SU(3)_f$  symmetry has been widely used in the hadron weak decays [4–16]. For  $\mathbf{B}_c \rightarrow \mathbf{B}^*M$ , there exist four parameters  $a_8$  and  $a_{9,10,11}$  [4, 6], which correspond to the decomposition of  $\mathcal{H}_{eff} = H(6) + H(\overline{15})$  in the  $SU(3)_f$  representation of 6 and  $\overline{15}$ , respectively. By comparison, we derive that

$$(E_{\mathbf{B}}, E_M) = (-2a_8 + a_9, 2a_8 + a_9), (E', C') = (-2a_9 - 2a_{10}, -2a_{11}), \quad (19)$$

such that  $a_i$  are found to correspond to the topologies. Since  $(E', C')$  have been the vanishing topological parameters, one has  $a_9 = -a_{10}$  and  $a_{11} = 0$ . Moreover, our global fits for  $E_{\mathbf{B},M}$  indicate that  $a_{9(10)}$  from  $H(\overline{15})$  has a non-zero value. By contrast, the numerical analysis performed with the irreducible  $SU(3)_f$  symmetry neglects the contributions from  $H(\overline{15})$  [7], whose results are given in the tables. In the physical mass scenario ( $S_{pm}$ ) for the global fit in Ref. [7], where  $m_{\mathbf{B}_c}$ ,  $m_{\mathbf{B}^*}$  and  $m_M$  are taken from the physical values in Ref. [1],  $\mathcal{B}(\Lambda_c^+ \rightarrow \Sigma^{*+}\eta, \Xi^{*0}K^+)$  and  $\mathcal{B}(\Xi_c^0 \rightarrow \Omega^-K^+)$  are fitted to be a few times smaller than the observations. Instead of considering the  $SU(3)_f$  symmetry breaking, one performs another fit in the equal mass scenario ( $S_{em}$ ), where  $m_{\Lambda_c} = m_{\Xi_c}$ ,  $m_{\Delta} = m_{\Sigma^*} = m_{\Omega}$  and  $m_{\pi} = m_{\eta} = m_K$ , resulting in the raised values of the above branching fractions.

#### IV. CONCLUSIONS

In summary, we have studied the  $\mathbf{B}_c \rightarrow \mathbf{B}^*M$  decays in the quark-diagram scheme. We have found that only two  $W$ -exchange diagrams,  $E_{\mathbf{B}}$  and  $E_M$ , could give contributions to the observed branching fractions of  $\Lambda_c^+ \rightarrow (\Delta^{++}K^-, \Sigma^{*+}\eta, \Xi^{*0}K^+)$  and  $\Xi_c^0 \rightarrow \Omega^-K^+$ . In addition, we have predicted  $\mathcal{B}(\Lambda_c^+ \rightarrow \Sigma^{*0(+)}\pi^{+(0)}) = (2.8 \pm 0.4) \times 10^{-3}$ , which respects the isospin symmetry. To interpret the observation of  $\mathcal{B}(\Lambda_c^+ \rightarrow \Sigma^{*+}\eta)$ , we have taken into account the  $SU(3)_f$  symmetry breaking. In particular,  $\mathcal{B}(\Lambda_c^+ \rightarrow \Delta^{++}\pi^-, \Xi_c^+ \rightarrow \Delta^{++}K^-) = (7.0 \pm 1.4, 13.5 \pm 2.7) \times 10^{-4}$  and  $\mathcal{B}(\Xi_c^+ \rightarrow \Delta^{++}\pi^-, \Xi_c^0 \rightarrow \Delta^-\pi^+) = (7.8 \pm 1.6, 2.5 \pm 0.4) \times 10^{-5}$  have been predicted as the largest branching fractions in the SCS  $\Lambda_c^+(\Xi_c^+)$  and DSC  $\Xi_c^{+(0)}$  decay channels, respectively.

## ACKNOWLEDGMENTS

We would like to thank Prof. X.G. He for useful discussions. This work was supported by National Science Foundation of China (11675030).

---

- [1] M. Tanabashi *et al.* [Particle Data Group], Phys. Rev. D **98**, 030001 (2018).
- [2] A. Zupanc *et al.* [Belle Collaboration], Phys. Rev. Lett. **113**, 042002 (2014).
- [3] M. Ablikim *et al.* [BESIII Collaboration], Phys. Rev. Lett. **116**, 052001 (2016).
- [4] M.J. Savage and R.P. Springer, Phys. Rev. D **42**, 1527 (1990).
- [5] M.J. Savage, Phys. Lett. B **257**, 414 (1991).
- [6] C.Q. Geng, Y.K. Hsiao, C.W. Liu and T.H. Tsai, JHEP **1711**, 147 (2017).
- [7] C.Q. Geng, C.W. Liu, T.H. Tsai and Y. Yu, Phys. Rev. D **99**, 114022 (2019).
- [8] X.G. He, Y.K. Hsiao, J.Q. Shi, Y.L. Wu and Y.F. Zhou, Phys. Rev. D **64**, 034002 (2001).
- [9] H.K. Fu, X.G. He and Y.K. Hsiao, Phys. Rev. D **69**, 074002 (2004).
- [10] Y.K. Hsiao, C.F. Chang and X.G. He, Phys. Rev. D **93**, 114002 (2016).
- [11] J. Pan, Y.K. Hsiao, J. Sun and X.G. He, Phys. Rev. D **102**, 056005 (2020).
- [12] C.D. Lu, W. Wang and F.S. Yu, Phys. Rev. D **93**, 056008 (2016).
- [13] C.Q. Geng, Y.K. Hsiao, Y.H. Lin and L.L. Liu, Phys. Lett. B **776**, 265 (2017).
- [14] C.Q. Geng, Y.K. Hsiao, C.W. Liu and T.H. Tsai, Phys. Rev. D **97**, 073006 (2018).
- [15] C.Q. Geng, Y.K. Hsiao, C.W. Liu and T.H. Tsai, Phys. Rev. D **99**, 073003 (2019).
- [16] Y.K. Hsiao, Y. Yu and H.J. Zhao, Phys. Lett. B **792**, 35 (2019).
- [17] H.J. Zhao, Y.L. Wang, Y.K. Hsiao and Y. Yu, JHEP **2002**, 165 (2020).
- [18] H.Y. Cheng and C.W. Chiang, Phys. Rev. D **86**, 014014 (2012).
- [19] H.n. Li, C.D. Lu and F.S. Yu, Phys. Rev. D **86**, 036012 (2012).
- [20] H.n. Li, C.D. Lu, Q. Qin and F.S. Yu, Phys. Rev. D **89**, 054006 (2014).
- [21] H.Y. Cheng and C.W. Chiang, Phys. Rev. D **100**, 093002 (2019).
- [22] Q.P. Xu and A.N. Kamal, Phys. Rev. D **46**, 3836 (1992).
- [23] J.G. Korner and M. Kramer, Z. Phys. C **55**, 659 (1992).
- [24] K.K. Sharma and R.C. Verma, Phys. Rev. D **55**, 7067 (1997).
- [25] Y. Kohara, Phys. Rev. D **44**, 2799 (1991).

- [26] L.L. Chau, H.Y. Cheng and B. Tseng, Phys. Rev. D **54**, 2132 (1996).
- [27] X.G. He, Y.J. Shi and W. Wang, Eur. Phys. J. C **80**, 359 (2020).
- [28] A.J. Buras, hep-ph/9806471.
- [29] T. Feldmann, P. Kroll and B. Stech, Phys. Rev. D **58**, 114006 (1998); Phys. Lett. B **449**, 339 (1999).
- [30] Y.K. Hsiao, L. Yang, C.C. Lih and S.Y. Tsai, arXiv:2009.12752 [hep-ph].
- [31] K. Miura and T. Minamikawa, Prog. Theor. Phys. **38**, 954 (1967); J.G. Korner, Nucl. Phys. B **25**, 282 (1971); J.C. Pati and C.H. Woo, Phys. Rev. D **3**, 2920 (1971).
- [32] Y.B. Li *et al.* [Belle Collaboration], Phys. Rev. D **100**, 031101 (2019).